5th International Conference on Experimental Fluid Mechanics – ICEFM 2018 Munich
Munich, Germany, July 2-4, 2018

Developing quantitative information of oil droplets rising through a rectangular confinement

Hirad Soltani[1], Reza Azadi[1], Aleksey Baldygin[1],

Shadi Ansari[1], David S. Nobes[1*]

[1]University of Alberta, Department of Mechanical Engineering, Edmonton, Canada

*dnobes@ualberta.ca

Abstract

Flow of an oil droplet in a net fluid co-flow through a vertical rectangular confinement is investigated in this study. Oil-in-oil emulsion can lead to coalescence of fine droplets forming into relatively larger droplets that need to be investigated individually. Emulsion can occur in a variety of industrial processes, where the effect of both body forces and surface forces should be considered. Here, the passage of a single oil droplet through a 3 mm × 5.84 mm (width × thickness) rectangular confinement, where the oil droplet diameter is relatively larger than the confinement width (3 mm), is monitored. A particle shadow velocimetry (PSV) system is employed as the optical measurement technique to capture the fluid flow motion inside and around the oil droplet as rising through the confinement. Transparent canola oil was used as the oil droplet and glycerol was chosen as the working fluid, allowing matching of the refractive index of both phases. The velocity field around and inside oil droplets were determined using a particle image velocimetry (PIV). Near the confining walls, PIV interrogation windows can potentially overlap with the wall or different flow features. In order to increase the resolution of the measurement, particle tracking velocimetry (PTV) image processing was assessed here. In PTV processing, since the particles are tracked individually (no interrogation window), sparse data sets are generated. To allow comparison of the two approaches, the PTV sparse data field was interpolated onto a regular grid and compared to PIV. While good general agreement was achieved, the spatial averaging of PIV resulted in a smoother vector field while noise was evident in the PTV as a result of the limits of particle detection inherent to the approach.

1 Introduction

Fluid particles, such as oil droplets, are important and applicable in many industries. Dispersion of liquid droplets in a fluid medium improves the mass transfer between the droplet and fluid medium, which is the base of fluid-fluid separation or separating liquid components of a multiphase solution (Komrakova, Eskin, and Derksen 2013). In liquid-liquid extraction processes, groups of liquid droplets are typically injected into the solution and hence the droplets would interact with each other. However, understanding the flow behavior of single oil droplets helps to study other types of droplet flow, such as flow of several droplets rather than single ones. Several forces are exerted on a droplet as it moves in a fluid medium, which are classified as surface forces and body forces that act on the droplet surface and volume of droplet respectively. For a moving oil droplet, main body forces are buoyancy, gravity and drag force, and surface forces are surface tension, viscous and surface charge forces (Kulkarni and Joshi 2005).

Many studies have been performed experimentally investigating of rising path, rising velocity, drag coefficient and shape oscillation of oil droplets as moving in an infinite fluid medium (Bäumler et al. 2011; Eiswirth et al. 2011; Thorsen, Stordalen, and Terjesen 1956; Wegener, Kraume, and Paschedag 2009). However, experimental investigation of flow inside and around an oil droplet rising in a fluid medium can be challenging due to the difficulties in running experiments for such a system (Ninomiya and Yasuda 2006) and the potential problems of light scattering at the droplet interface. Comparison of the experimental results may not be valid, mainly because of difficulties in addressing the impurities in the fluids (Wegener, Kraume,

and Paschedag 2009). As a result, mostly numerical approaches have been undertaken to investigate the flow pattern inside and around a rising/falling oil droplets in a fluid medium and the results were validated with empirical correlations and/or collecting experimental data (Bäumler et al. 2011; Eiswirth et al. 2011; Komrakova, Eskin, and Derksen 2013).

In this study, in order to avoid potential illumination issues that might ensue by using a standard particle image velocimetry (PIV) approach, a particle shadow velocimetry (PSV) setup is used to investigate the flow inside and around a canola oil rising in a glycerol continuous phase. This paper quantifies the fluid flow of oil droplets as the fluid and droplets flow in a vertical narrow straight slot in the opposite direction of gravity. PIV was employed to process data images and quantify the velocity field around and inside the oil droplet. Near the confining wall region, the PIV interrogation windows might overlap and perhaps deteriorate the measurement resolution. Therefore, particle tracking velocimetry (PTV) was used to increase resolution here and the results are compared to PIV. This experiment was carried out for one bulk flow rate and one droplet of larger size relative to the confinement width was generated to investigate the effect of confining wall on the flow inside the oil droplet near the walls.

2 Experimental Setup

An experimental setup was developed in such a way as to allow investigation of the velocity field around and inside a single oil droplet rising through a vertical rectangular confining geometry. The configuration allowed the passage of the droplet through a vertical confinement designed inside a flow channel. In this study, the bulk flow rate is addressed as fluid flux, which is defined as:

$$q = Q/A \tag{1}$$

where q is the fluid flux, Q is the volumetric flow rate and A is the cross-sectional area. Here, one fluid flux of 2.64 mm/s for the bulk flow was provided to flow along with the droplets. Even though matching refractive index (RI) is a more important than viscosity, the viscosity of the bulk fluid should still be relatively high to provide a creeping flow regime. In this experiment, transparent canola oil was used as the droplet and 100 Wt% glycerol was employed as the working fluid, which are immiscible fluids. The refractive index (RI) of canola oil and glycerol were measured as 1.4730 and 1.4723 respectively (Abbe-3L, Bausch and Lomb). The canola oil viscosity was measured as 0.0738 kg/(ms), using a rotational rheometer (Rheolab QC, Anton Paar GmbH) with double gap measuring cup (DG42, Anton Paar GmbH). The density of the canola oil was also measured as 915 kg/m^3 using a force tensiometer (K100, KRUSS Scientific Instruments, Inc.) with the measuring probe for density measurements (DE0601, KRUSS Scientific Instruments Inc.). The glycerol properties for density (1261 kg/m^3) and dynamic viscosity (1412 kg/(m.s)) were acquired from the literature (Segur and Oberstar 1951; Trejo González, Longinotti, and Corti 2011).

Microbeads particles (Dynoseeds® TS 10, Microbeads Skedsmokorset, Norway) of 10 µm size and 1050 kg/m^3 density were mixed in the canola oil and glycerol as the tracer particles before injecting into the flow channel. After mixing the tracer particles into the droplet and working fluids, the solution was left stationary for 48 hours to separate particles of relatively heavier and lighter weight than the fluid. The mixture of the fluid and tracer particles at the middle of the solution was used to be injected into the system. This resulted in tracer particles of 1 to 3 pixels in size in the images captured in the experiment.

A PSV, or back-light illumination approach was employed to capture the motion of droplets rising through the flow cell. Figure 1 shows a schematic of a shadowgraph setup for the experiments. The optical setup contained a high speed camera (CMOS SP - 5000M – PMCL, JAI Inc.) with 2560 pixel × 2048 pixel resolution capable of capturing up to 134 frames-per-second along with a macro lens (Sigma 105 mm f/2.8 EX DG) and an LED (BX0404, Advanced Illumination Inc.) source to provide illumination. The camera was operated with an exposure time of 360 µs to freeze the droplet motion and camera frame rate was controlled using a function generator (AFG3021B, Tektronics Inc.). The LED source was aligned on the same optical axis as the camera at the back of flow cell to provide uniform illumination over the region of

interest. The experimental configuration provided a field of view (FOV) of 8 mm × 9 mm to investigate the flow inside and around droplets.

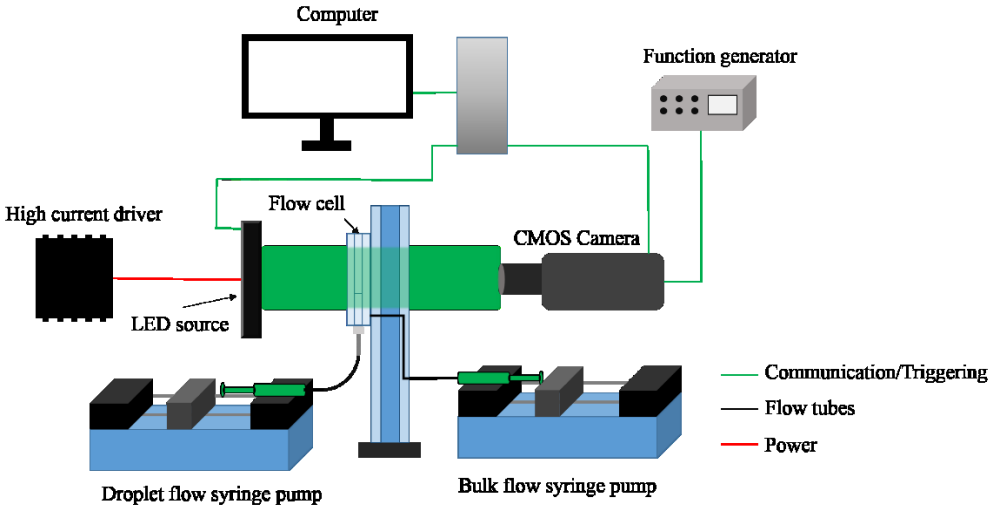

Figure 1: The schematic of the shadowgraph experimental setup

Figure 2(a) shows the 60 mm × 250 mm flow cell design, which consisted of a flow channel and two PMMA side windows confining the flow channel and developing the required rectangular shape. The flow channel of 5.84 mm depth (Optix Acrylic; Plaskolit Inc.) was manufactured using a commercial laser cutter (VersaLaser VLD Version 3.50; Universal Laser Systems) which provided flexibility in shaping the geometry of the flow channel. As shown in Figure 2(a), an inlet orifice of 4 mm diameter was used to inject the working fluid into the flow channel via the rear window relative to the camera view and a similar orifice was used for flow outlet. An inlet tube was connected to a syringe which was mounted on a syringe pump (‘11’ Plus, Harvard Apparatus Inc.). Oil was injected through a nozzle into the fluid medium to create a droplet. Figure 2(b) shows the different flow regions in the flow cell including a parallel plate region (PPR) (22 mm × 5.84 mm, width × thickness) before and after a rectangular cross sectional region (RCSR) (3 mm × 5.84 mm, width × thickness). The flow cell was mounted vertically in the experimental setup and the bulk flow direction was opposite to gravity.

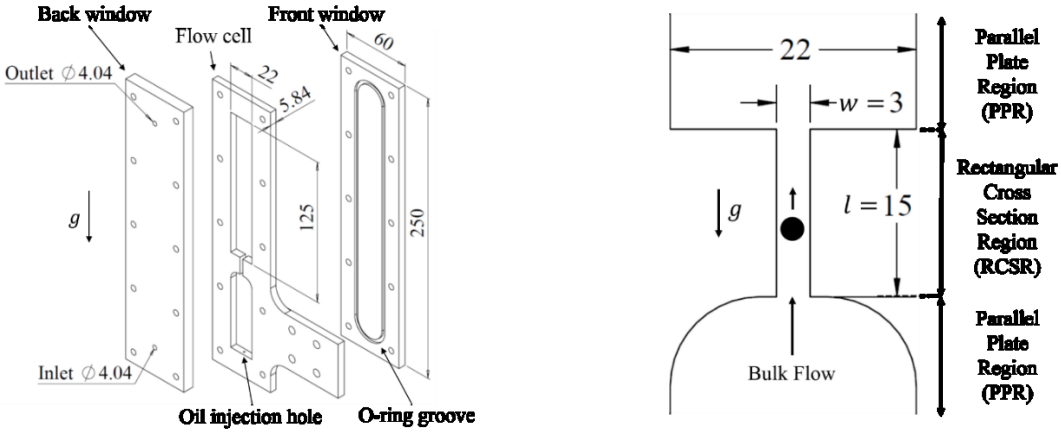

(a) (b)

Figure 2: Flow cell design for investigating flow around and inside oil droplets; (a) a disassembled solid model of the flow channel, (b) details of the two-dimensional flow geometry, which has a constant depth of 5.84 mm. All dimensions are in mm

3 Image Processing Approaches

To determine the relative velocity in the surrounding fluid medium both PIV and PTV analysis of the seed particles were undertaken. For PIV processing (Davis 8.4.0, LaVision GmbH), image intensity was inverted so that tracer particles became bright and more distinct. A "subtract sliding background" option was used to eliminate non-uniform light intensity. A set value was subtracted from the intensity of the whole image to make the intensity of most parts of the background closer to zero. Multi-pass cross correlation with decreasing interrogation window size processing scheme was utilized to determine the velocity field in the bulk flow. A large interrogation window of 128 pixel × 128 pixel was chosen to capture large changes in the velocity field followed by a 64 pixel × 64 pixel window. First and second interrogating windows were used with three and one passes respectively, and 75 % window overlap in between sequential correlations.

PTV image processing, that takes into account the time resolve nature of the data collected, was conducted using a commercial software (Davis 8.4.0, LaVision GmbH). In this processing, every tracer particle is tracked individually over time. Hence, after detecting each particle and eliminating the background noise, particles can be tracked in between sequential frames and results will be in the form of a sparse field of velocity vectors at the highest possible particle resolution. In PTV pre-processing, images were inverted similar to PIV pre-processing and a "subtract sliding background" and Gaussian smoothing operations were undertaken on the images to minimize noise. In this study, by trial and error, the particles was chosen to be tracked over 5 frames to have a desired velocity vector resolution. In PTV processing, typically, tracking particles over more frames gives more confidence in the results. However, by tracking particles over a larger number of frames, some of the particles can disappear and hence the number of tracked particles can decrease, lowering the number of available vectors for analysis. The spatial coherence of the velocity vectors were also checked to the vectors in the neighborhood. The sparse vector field can then be mapped onto a regular grid of results for the determination of other parameters.

4 Results and Discussion

For a system of rising droplets, the reference frame can be set at a fixed location (Eulerian frame) to observe the absolute motion of droplet, or on the center of the rising droplet to see the movement of droplet relative to the surroundings (Lagrangian frame). The velocity field from PIV and PTV processing are shown for some example images in Figure 3. In the figure, the black arrows represent the velocity vectors, V is the velocity magnitude and x and y are respectively the horizontal and vertical locations normalized by the RCSR width, w where the points -0.5 and 0.5 on the x-axis represent the left and right sides of the RCSR.

In Figure 3, the velocity vectors are plotted for every 1 and 6 vectors in the x and y directions, respectively, for PIV processed data (Figures 3(a) and 3(d)). However, in PTV data field, the velocity vectors are plotted for every 3 and 18 vectors in the x and y directions (Figures 3(c) and 3(f)). Figure 3(a) plots the PIV velocity vectors on a colour map background in Eulerian reference frame. In Figure 3(b), the PTV vector field highlights the sparse nature of the velocity vectors, a result of which is that a colour map velocity background cannot be directly plotted. For PTV data there are some regions with no velocity vector, because no tracer particle was detected. To allow a comparison, the PTV data was interpolated and mapped onto a regular grid with 5 pixels resolution, the results of which are shown in an Eulerian reference frame in Figure 3(c).

To observe the fluid motion inside the droplet relative to the surrounding fluid, a value close to the droplet terminal velocity was subtracted from the whole velocity field. Figures 3(d-f), which plot the velocity vectors under laid by the vorticity in Lagrangian frame, show that there are two counter-rotating vortices on either sides of the droplet near the confining walls. This flow motion occurs because of the force exerted on the droplet from the surrounding fluid and the confining walls. As shown in Figures 3(d) and (f), the local velocity of the fluid is relatively higher inside the droplet comparing to the other regions. This is because the droplet terminal velocity is higher relative to the fluid co-flow and the region around the droplet center is at the RCSR centerline, which is farthest from the confining walls. Comparison of PIV and PTV velocity vectors indicate that a relatively higher velocity vector resolution is derived from PTV processing.

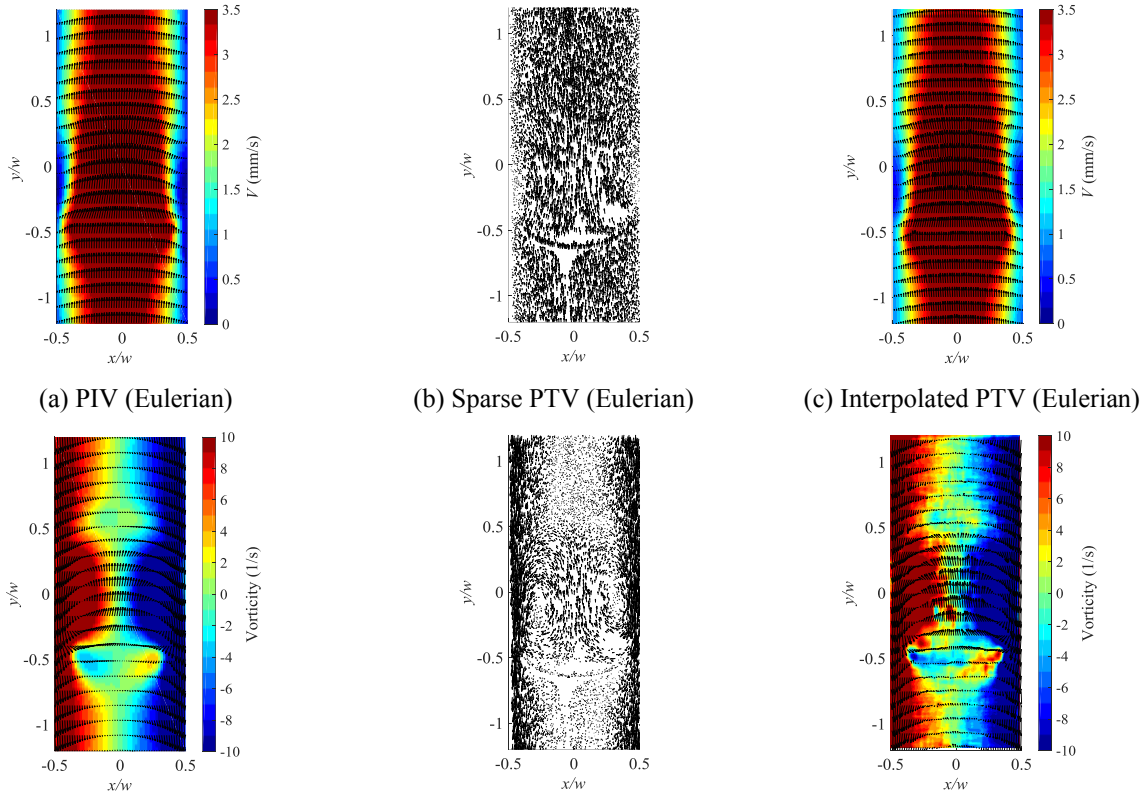

(a) PIV (Eulerian) (b) Sparse PTV (Eulerian) (c) Interpolated PTV (Eulerian)

(d) PIV (Lagrangian) (e) Sparse PTV (Lagrangian) (f) Interpolated PTV (Lagrangian)

Figure 3: Examples of velocity field from PIV and PTV processing for a relatively large oil droplet, where the velocity vectors are plotted for every 1 and 3 vectors in the horizontal direction for PIV and PTV data respectively

Figures 4(a) and 4(b) show a zoomed-in image of the data shown in Figures 3(d) and 3(f), respectively, to demonstrate the vorticity map at the leading edge of the droplet in more detail. In Figures 4(a) and 4(b), the velocity vectors density in the vertical and horizontal directions is the same as Figures 3(d) and 3(f) respectively. Comparison of PIV and PTV processed data in Figures 4(a) and 4(b) shows the PTV data provides a relatively higher velocity vector resolution, because in PIV processing, the particles displacement are averaged over the interrogation windows and only one velocity vector is calculated per window. This might lead to decrease in the velocity vector resolution and hence, losing the details of the fluid flow. In PTV processing, however, particles are tracked individually in flow field and a relatively higher velocity vector resolution can be derived. Therefore, more details of the fluid flow can be derived.

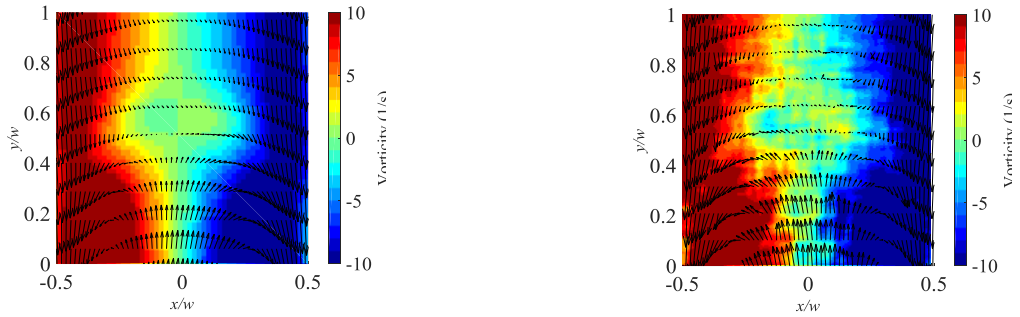

(a) PIV (b) PTV

Figure 4: Examples of vorticity field from (a) PIV, and (b) PTV processing in Lagrangian reference frame, where the velocity vectors are plotted for every 1 and 3 vectors in the horizontal direction for PIV and PTV data

4 Conclusion

The flow around and inside a relatively large oil droplet rising through a rectangular confinement has been experimentally investigated. PIV and PTV were employed to analyze the displacement of tracer particles in the flow around and inside the rising oil droplets. Qualitatively, it was shown that the PIV and PTV processing approaches give approximately the same result; however, more details of the flow was observed in the PTV processed data, compared to PIV velocity field. This is because in PIV processing, the particles displacement is averaged over the interrogation windows. However, in PTV processing, the particles are tracked individually which might lead to relatively higher velocity vector resolution in the data.

Acknowledgements

The authors gratefully acknowledge financial support from Natural Sciences and Engineering Research Council (NSERC) of Canada, the Alberta Ingenuity Fund, the Canadian Foundation for Innovation (CFI) and RGL Reservoir Management Inc.

References

Bäumler K, Wegener M, Paschedag AR, and Bänsch E (2011) Drop Rise Velocities and Fluid Dynamic Behavior in Standard Test Systems for Liquid/liquid Extraction-Experimental and Numerical Investigations. *Chemical Engineering Science* 66: 426–39.

Eiswirth RT., Bart HJ, Atmakidis T, and Kenig EY (2011) Experimental and Numerical Investigation of a Free Rising Droplet. *Chemical Engineering and Processing: Process Intensification* 50: 718–27.

Komrakova AE, Eskin D, and Derksen JJ. (2013) Lattice Boltzmann Simulations of a Single N-Butanol Drop Rising in Water. *Physics of Fluids* 25: 42102.

Kulkarni AA, and Jyeshtharaj BJ (2005) Bubble Formation and Bubble Rise Velocity in Gas - Liquid Systems : A Review. *Industrial & Engineering Chemistry Research* 44: 5873–5931.

Ninomiya N., and Yasuda K. (2006) Visualization and Piv Measurement of the Flow around and inside of a Falling Droplet. *Journal of Visualization* 9(3): 257–64.

Segur, JB, and ,Oberstar EH. 1951. Viscosity of Glycerol and Its Aqueous Solutions. *Industrial & Engineering Chemistry* 43(9): 2117–20.

Thorsen G, Stordalen RM, and Terjesen SG (1956) On the Terminal Velocity of Circulating and Oscillating Liquid Drops. *Chemical Engineering Science* 2: 444–47.

González, José AT, Longinotti MP, and Horacio RC (2011). The Viscosity of Glycerol-Water Mixtures Including the Supercooled Region. *Journal of Chemical and Engineering Data* 56(4): 1397–1406.

Wegener M, Kraume M, and Paschedag AR (2009) Droplet Microfluidics on a Planar Surface. *Fluid Mechanics and Transport Phenomena* 56: 2–10.